

Optimization of molecularly thin lubricant to improve bearing capacity at the head-disk interface

Shahla Chowdhury · Antonis I. Vakis ·
Andreas A. Polycarpou

Received: 11 May 2014 / Accepted: 5 November 2014 / Published online: 25 November 2014
© Springer-Verlag Berlin Heidelberg 2014

Abstract A molecularly thin lubricant layer (of the order of 1–2 nm thick) has been shown to provide bearing forces at the interface between contacting solid surfaces under light loads and high shear rates. This phenomenon is important, for example, in the head-disk contact in magnetic storage hard disk drives to ensure that some of the contact is sustained by the lubricant layer and thus avoiding damage of the solid surfaces. The magnitude of the normal and tangential bearing forces that the lubricant layer can provide depends on temperature, viscosity of the lubricant, sliding velocity and radius of gyration of the lubricant molecules. This study shows that viscosity has the greatest effect on the load bearing capacity of the molecularly thin lubricant. Thus, by controlling the flash temperature and the ratio of molecularly thin lubricant-to-bulk viscosity, the bearing load carrying capacity of the layer can be controlled. This would allow for the contact to be sustained within the mobile lubricant layer, avoiding solid contact so as to protect the diamond-like carbon coating, and thus reduce wear and potential catastrophic failures.

1 Introduction

It is important to bring the read/write elements of the recording head at a head disk interface (HDI) of a hard disk-drive (HDD) as close as possible to the disk surface to achieve the highest possible recording density. For a recording density of 1 Tbit/in², the magnetic clearance (the distance between the read/write elements and the disk magnetic layer) must be reduced to below 6.5 nm (Wood 2002). One of the main engineering barriers in attaining Tbit/in² areal densities lies in the area of interfaces, specifically achieving the necessary physical clearance between the slider and disk surfaces (Suh and Polycarpou 2008). To increase the operational life of HDDs, it is important to avoid contact between the slider and disk surface. Contact recording, with the slider physically approaching and dragging on the disk surface during operation, could yield the minimum practical clearance. However, contacting the disk surface is not desirable as it results in vibrations and wear; research also indicated that due to high interfacial adhesion combined with a shock event can also lead to slider/head crashes (Lee and Polycarpou 2005). Thermal fly-height control (TFC) technology was introduced to avoid dynamic instabilities observed with sub-5-nm clearances. TFC uses a thermal element to create a protrusion or bulge around the read/write elements of the slider and bring them close to the rotating disk surface, while the slider body remains flying nominally at about 10 nm (Vakis et al. 2009).

To minimize wear of the slider and disk due to contact and also to protect against corrosion, a very thin layer (~1–1.5 nm) of perfluoropolyether (PFPE) lubricant is used over the Diamond-Like Carbon (DLC) coating. Customarily, molecularly thin lubricant (MTL) contact has been neglected in rough surface contact and sliding models (Lee and Strom 2008) by assuming that the lubricant is

S. Chowdhury · A. I. Vakis · A. A. Polycarpou (✉)
Department of Mechanical Science and Engineering, University
of Illinois at Urbana-Champaign, Champaign, IL 61801, USA
e-mail: apolycarpou@tamu.edu

S. Chowdhury · A. A. Polycarpou
Department of Mechanical Engineering, Texas A&M University,
College Station, TX 77843, USA
e-mail: chowdhury.s@tamu.edu

A. I. Vakis
Faculty of Mathematics and Natural Sciences, University
of Groningen, 9747 AG Groningen, The Netherlands
e-mail: a.vakis@rug.nl

readily displaced upon slider-disk contact. A rough surface model of MTL contact was proposed by Vakis and Polycarpou (2012), where the model builds on a single asperity model (Vakis et al. 2011) that accounts for dynamic shearing experiments with polymeric thin lubricants (Fukuzawa et al. 2009; Vakis and Polycarpou 2010), and is coupled with an existing rough surface dynamic contact model with friction (Suh and Polycarpou 2005). The MTL model has also been extended to include variable lubricant surface energy (Yeo et al. 2008; Suh et al. 2006; Vakis and Polycarpou 2013).

In MTL films, a parameter called chain stiffness would be relevant in the formulation of an improved tribological model for lubricant contact (Guo et al. 2012; Hiroshi and Tagawa 2012), as would be relaxation and creep phenomena (Karis 2009); however, the present improved molecularly thin lubricant model (IMTL) (Vakis and Polycarpou 2013) does not rely on physics-based derivations of lubricant rheology. Instead, the IMTL is a semi-empirical model that utilizes experimental measurements of the behavior of molecularly thin lubricant layers under extremely high shear rates (Fukuzawa et al. 2009) to predict an equivalent stiffness for the MTL layer in the normal and shear directions. These experimental measurements yield the complex viscosity as a function of separation and utilize continuum fluid dynamics to characterize shear-induced (Couette) flow. Marchon and Saito (2009) reported that the fluid behavior could be modeled reasonably well using Poiseuille flow. Since MTL films behave as glassy solids at the extremely high shear rates encountered in magnetic storage, as was rightly pointed out by the reviewer, the IMTL model uses the shear-rate-varying force predictions from continuum fluid dynamics (Couette formulation for the shear and Kapitza formulation for the normal force) and calculates the layer's effective stiffness as the partial derivative of the force with respect to separation. The morphological properties of MTL films were also accounted for in earlier work (Vakis et al. 2011, 2012; Vakis and Polycarpou 2012) where a limit was acknowledged for the applicability of continuum formulations. Specifically, continuum fluid dynamics were utilized as described above up to the point where the shear rate within the lubricant film 'vanishes' once mobile lubricant molecules will have been expelled from the contacting interface. It is assumed that the maximum shear and normal stiffness of the MTL film will have been reached at this point and that lubricant stiffness (i.e., resistance to shearing and compression) would tend to be zero during the inception of solid (asperity) contact. In the present work, the effects of temperature and humidity to the measured viscosity have been accounted for, and as such, the predictions of the effective stiffness of the MTL layer have been improved.

Cho et al. (1997) performed experiments, which proved that the MTL viscosity is different from that of the bulk viscosity. To quantify these differences between bulk and thin-film viscosity, they developed an instrument to measure the shear of parallel single crystal solids separated by MTL films (Fisher and Israelachvili 1979). The effective shear viscosity is enhanced compared to the bulk, relaxation times are prolonged and nonlinear responses set in at lower shear rates. From another experimental investigation it has been reported that exceptionally low energy dissipation is possible when fluids move past solid surfaces that are sufficiently smooth (Zhu and Granick 2004). Molecular dynamics (MD) simulations have shown that wall interaction and molecular end-group functionality affect the behavior of the lubricant layer, while lubricant confinement (separation between the solid surfaces) and shear rate were found to play a critical role in determining the lubricant's liquid- or solid-like responses (Demirel and Granick 1998). Furthermore, MD simulations have shown that there is a transition that tends to nucleate in distorted or imperfect regions in the lubrication film (Persson 1997), which they term as squeeze-out region. This transition is due to molecular layering: When the contact is at a single molecular layer, then the squeeze out starts. Thus the two different regimes in the MTL model are qualitatively validated from experimental evidence and MD simulations. The first regime is a hydrodynamic contact regime with the mobile lubricant layer, which behaves as a semi-solid at high shear rates, and the second regime is the squeeze-out or rupture of the bonded lubricant molecules, resulting in the initiation of solid contact.

The variation of surface energy is important for nanoscale contacts such as the ones under consideration. The IMTL model used in our calculations utilizes experimental measurements of surface energy (Yeo et al. 2008) as a function of the separation between the solid surfaces and hence, penetration of the slider into the lubricant layer; however, its variation with temperature and humidity was not accounted for in the present work due to the lack of relevant experimental data. Furthermore, interfacial adhesion is arguably more important within the dynamical context of bringing the surfaces into contact at sub-5-nm clearances and less so during lubricant contact (Vakis and Polycarpou 2012).

In the presence of MTL layers, the sub-boundary lubrication (SBL) model (Stanley et al. 1990) is used to account for the adhesive forces. As the disk surface in a HDD is atomically rough, the lubricant thickness reaches a critical point (when adhesion increases rapidly) at very small lubricant thickness (Muller et al. 1980). Adhesive interactions are modeled by a Lennard-Jones surface potential (Mate et al. 1989), since a large amount of energy is

associated with the formation of a unit area of solid-lubricant interface, and the energy cost of liquid bridge formation is too high and meniscus formation is energetically unfavorable (Muller et al. 1980). The adhesive force and pull-off force are highest for the smoother interface and separations below 2 nm (Yeo et al. 2008). Experimental work also showed that the surface energy of MTL layers on solid substrates is not constant but varies with penetration into the lubricant layer (Suh and Polycarpou 2005). The MTL model has been extended to account for surface roughness (Kogut and Etsion 2004), which is modeled using an extension of the statistical Greenwood-Williamson (GW) formulation (which also accounts for elastic-plastic contact).

The MTL model however does not account for the heating of the lubricant, which can be caused by flash temperature and viscous friction. Archard (1958) have shown that the temperature difference within the film is the largest transient temperature in the contact region and it may be more than five times greater than the solid surface flash temperature. The heat generated by one pair of contacting asperities has been shown to be extremely small; contrary to the flash temperature, viscous heating effects have proved to be extremely important (Wietzel 1993). Spikes and Olver (2009) observed that the heat generated from compression is very small in comparison to the heat caused by shearing under sliding conditions. Compared with iso-viscous models, significant reductions of film thickness and friction forces, especially in regions of high surface speeds, were observed beyond the predictions of conventional pressure-viscosity relationships. At high speeds, the rise in maximum temperature is more than 90 % for a mixed lubricated system and depends on the surface roughness and sliding speed (Deolalikar and Sadeghi 2008). Through the analysis of thermal effects on Z-DOL lubricant using TOF-SIMS analysis, it was found that when Z-DOL lubricant is heated during operation its temperature is higher than the operating temperature (Rong et al. 2008). The average local temperature at the contacting interface is typically experimentally measured using resistive temperature sensors in magnetic storage heads (Kunkel et al. 2014). Typical “normal” measured temperatures are below 90 °C, and in this work we have used a higher range to designate more aggressive contact conditions. Thus, from various experiments and modeling investigations, evidence is present regarding the MTL heating during operation.

Using the MTL formulation to account for maximum stiffness and bearing forces that the lubricant can sustain, in this work, we present a study using design-of-experiments/analysis-of-variance (DOE/ANOVA) methodologies (DeVor et al. 1992). The study is three-dimensional: three parameters (that affect lubricant stiffness), sliding velocity,

MTL viscosity and radius of gyration, are varied between three levels (−1, 0 and +1). The parametric study yields predictive models that can be used to determine the optimum combinations of these parameters that would give the maximum possible MTL lubricant bearing performance.

2 Rough surface with MTL modeling

The ISBL model (Suh and Polycarpou 2005; Vakis and Polycarpou 2010) does not account for the load bearing capacity of the lubricant, which was accounted for in the MTL model (Vakis et al. 2011). During operation, the head and disk can remain separated or can be in contact as shown in the overall HDD schematic in Fig. 1 and the HDI schematic in Fig. 2. According to the MTL model the semi-solid lubricant has two regimes of contact and follows the rough topography of the substrate, with 99.7 % of which is circumscribed within 3σ from the mean of surface heights (Vakis and Polycarpou 2010). The thickness

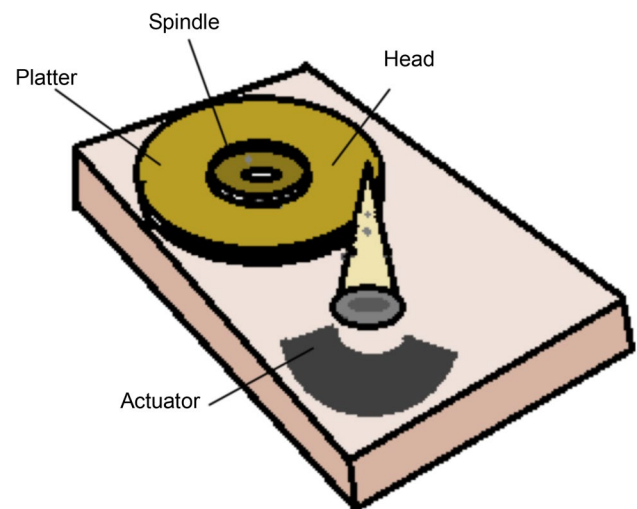


Fig. 1 Hard-disk-drive schematic

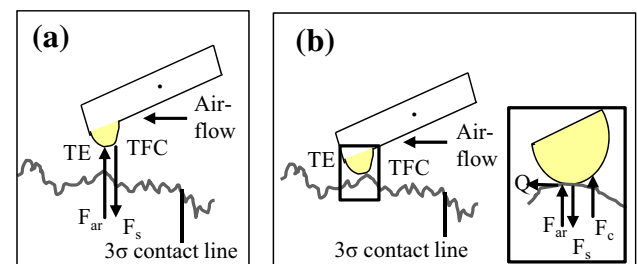


Fig. 2 Schematic of the HDI showing the relevant forces under a flying without contact and b contact conditions

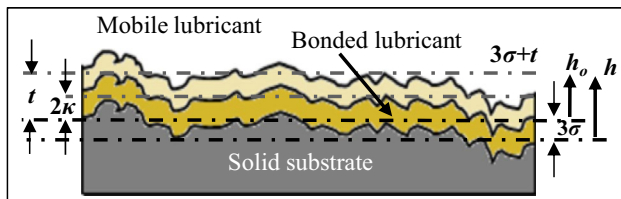


Fig. 3 Schematic of rough lubricated surface topography

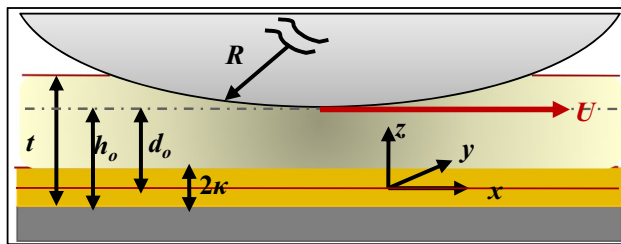


Fig. 4 Schematic of a rigid smooth sphere moving in a viscous fluid of thickness, t parallel to a plane (x -axis is at the center of the bonded lubricant)

of the MTL layer is t , of which the bonded thickness of the lubricant is considered to be equal to twice the radius of gyration, κ of the lubricant (Vakis and Polycarpou 2012). Thus, the total thickness of the bonded lubricant is 2κ and the thickness of the mobile lubricant layer is $t-2\kappa$ as shown in the schematic of Fig. 3. The roughness of the surface is accounted for using a statistical model: An equivalent rough surface composed of a statistically large number of spherical asperities of the same radius R and varying height according to a normal distribution, making contact with a rigid flat surface (Greenwood and Williamson 1966). The single asperity model, which is used as a ‘cell’ in the statistically rough surface model, is shown in Fig. 4.

In displacement control dynamic shearing experiments we observe three regimes of contact: (a) Steady lubricant contact (b) steady solid contact and (c) transition between the two regimes. Here ‘ h ’ is the separation between the mean of the surface heights of the two solids. We obtain the three regimes of contact by $3\sigma + 2\kappa \leq h < 3\sigma + t$, $3\sigma \leq h < 3\sigma + 2\kappa$ and $h < 3\sigma$ as shown in the schematic of Fig. 5. Here $h = h_0 + 3\sigma$, where h_0 is the solid–solid gap (Fig. 3). Under certain conditions, lubricant forces are maximized when the solid–solid gap becomes equal to 2κ ; after that the lubricant is considered to breakdown and become expelled from the substrate, providing almost no resistance (Damirel and Granick 1998), until solid contact is initialized. Research has shown that under very high shear rates and solid confinement, MTLs exhibit solid-like behavior (Vakis and Polycarpou 2010). Therefore MTL films under high shear rate would be expected to have measurable normal and shear stiffnesses.

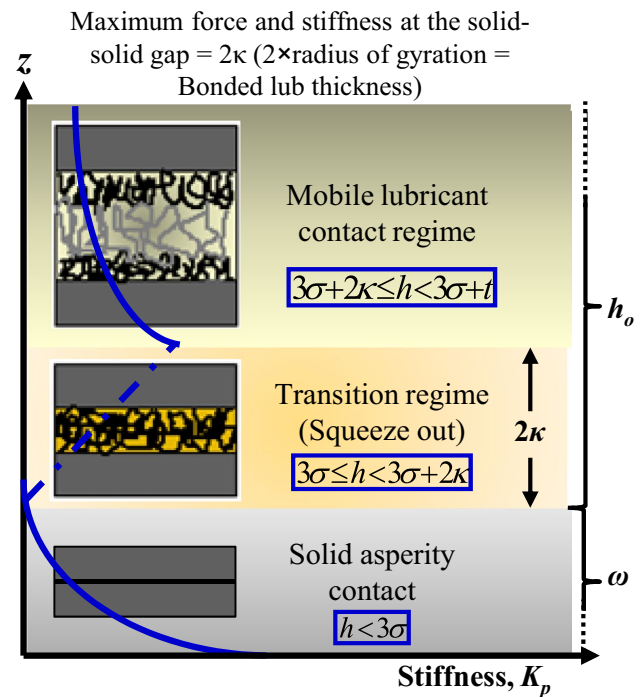


Fig. 5 Regimes of contact (the blue line indicates stiffness of the lubricant in different regimes)

Table 1 Disk and slider material and roughness properties (Vakis and Polycarpou 2010)

Symbol	Parameter	Value	Unit
E_{Disk}	Disk (DLC) Young’s modulus	280	GPa
ν_{Disk}	Disk (DLC) Poisson ratio	0.240	–
E_{TFC}	TFC Young’s modulus	280	GPa
ν_{TFC}	TFC Poisson ratio	0.240	–
H	Disk (DLC) hardness	13	GPa
$\Delta\gamma$	Surface adhesion energy	0.055	N/m
σ	Combined RMS roughness	0.36	nm
R	Combined mean radius of asperity curvature	0.276	μm
η	Combined areal density of asperities	0.270	μm^{-2}
R_o	Probe radius	102	μm

Table 2 Dynamic parameters of the slider and disk (Vakis and Polycarpou 2010)

Symbol	Parameter	Value	Unit
U_o	Experimental shearing velocity	200	$\mu\text{m/s}$
κ_o	Minimum liquid gap (disp. Ctrl)	102	μm
$\dot{\gamma} = U_o/\kappa_o$	Limiting shear rate	2×10^5	s^{-1}
M	Fitting coefficient	0.5	–
N	Fitting coefficient	1.46×10^{-7}	–
U	Sliding velocity at the HDI	21.8	m/s

The MTL model formulation is given in the “Appendices 1 and 2”. The disk and slider material and roughness properties are listed in Table 1 and the dynamic parameters are given in Table 2. These values were obtained from roughness, nanoindentation, and dynamic measurements (Vakis and Polycarpou 2010).

2.1 Temperature effect on viscosity

The confined MTL under high shear rates behaves differently than the bulk (Scarpulla and Mate 2003). Based on modeling work, we have found that the MTL viscosity is $5 \times -8 \times$ of the bulk viscosity at the operating temperature. Also, the bulk viscosity of the PFPE lubricant used in this study (Z-tetraol with a molecular weight of about 2,700) was measured at different temperatures. A cubic polynomial is fitted in natural log of bulk viscosity vs. natural log of temperature, as shown in Fig. 6. From this model, we can find the bulk viscosity of the lubricant at higher temperatures as needed. At different temperatures the lower and higher limit of MTL viscosity is calculated (considering $5 \times -8 \times$ of bulk viscosity) and maximum forces and stiffnesses at these limits are calculated using the MTL model, which is shown in Table 3.

As viscosity changes logarithmically with temperature, the range of MTL viscosity values ($5 \times -8 \times$ of bulk viscosity) is significantly larger for lower temperatures. With increasing temperature, this range decreases exponentially. Though the operating temperature of the HDD is 5–50 °C (Seagate Technology 2014; Scarpulla and Mate 2003), at the asperity level/contact it can be as high as 250 °C (Mate et al. 1989) due to flash temperatures. Also, a temperature hike of two to three times the operating temperature is observed, as a consequence of frictional heating (Wietzel 1993). Accounting for the effects of frictional heating and flash temperature, we assume that average local temperatures at the contact range between 90 and 120 °C. Consequently, the range of MTL viscosity is found to be

0.4 ± 0.2 Pa·s and the normal bearing force, calculated through the MTL model (using Eq. 5 in the “Appendix 1”), is 5.4 ± 2.6 mN. It is also apparent that both the temperature and the MTL/bulk viscosity ratio are very important in the calculation of the maximum bearing force. The shear force is calculated using Eq. 6 in the “Appendix 1” and the values are 2.7 ± 0.5 μN. The shear force is negligible in comparison to the normal bearing force. For the MTL viscosity range of 0.4 ± 0.2 Pa·s, the normal bearing stiffness is found to be 3.65 ± 1.85 N/μm.

An important phenomenon with the new lubricant property is that even at a temperature of 40 °C, the MTL stiffness value is reasonable, with a normal stiffness value corresponding to 0.82 nm of penetration into the solid substrate [stiffness = 50×10^6 N/m (Vakis et al. 2011)]. As shearing stiffness is not a function of viscosity (i.e., temperature and MTL viscosity ratio), its value is constant for a uniform radius of gyration of the lubricant. However the higher the radius of gyration is, the lower is the shearing stiffness (for, $\kappa = 0.73, 0.94$ nm; $Kq = 87.1, 67.64$ N/m, respectively). The measured lubricant properties are given in Table 4.

2.2 Parametric study

DOE/ANOVA methodologies were used to generate prediction models for the HDI system behavior using the improved MTL model and the obtained viscosity properties. A 3^3 full factorial design was implemented where three lubricant and operating parameters, μ, κ, U , were varied at three levels, $-1, 0,$ and $+1$. Using this methodology, any desired simulation output (response variable) could be analyzed (i.e., bearing and shear forces and normal and shear stiffnesses). The three levels of MTL viscosity (μ), radius of gyration (κ) and sliding velocity (U) corresponding to $-1, 0$ and $+1$ level values are given in Table 5.

To check the validity of the predictive models, residual analyses were performed whereby the residual errors were

Fig. 6 Experimentally measured bulk viscosity of PFPE at different temperatures; **a** linear plot; **b** the same data in logarithmic scales and fitted polynomial

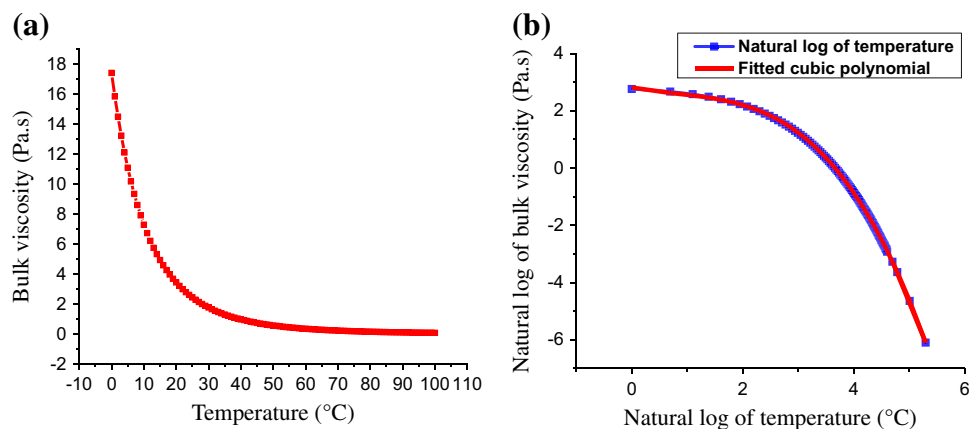


Table 3 Maximum forces and stiffnesses at different temperature values

	Maximum normal bearing force, P (mN)	Maximum shear force, Q (μ N)	Maximum bearing stiffness, K_p (N/ μ m)	Maximum shear stiffness, K_Q (N/m)
MTL/bulk viscosity ratio	$5 \times -8 \times$	$5 \times -8 \times$	$5 \times -8 \times$	$5 \times -8 \times$
Temperature ($^{\circ}$ C)				
40	82.81 ± 19.11	16.34 ± 3.36	56.72 ± 13.09	87.1 ± 0
60	28.45 ± 6.57	6.76 ± 1.15	19.49 ± 4.49	87.1 ± 0
80	11.08 ± 2.56	3.70 ± 0.45	7.59 ± 1.75	87.1 ± 0
100	4.58 ± 1.17	2.57 ± 0.19	3.20 ± 0.74	87.1 ± 0
120	2.30 ± 0.53	2.15 ± 0.09	1.57 ± 0.36	87.1 ± 0
150	0.84 ± 0.19	1.89 ± 0.04	0.58 ± 0.13	87.1 ± 0

Table 4 MTL (PFPE) properties

Symbol	Parameter	Value	Unit
T	Thickness of the MTL	1.1	nm
K	Radius of gyration	0.73 and 0.94	nm
BR	Bonding ratio	0.5 and 0.85	–
C	Coverage	80–85 %	–
μ_o	Limiting viscosity	0.2–0.6	Pas

Table 5 Values of μ , κ , U at three levels (-1 , 0 , $+1$)

	Level -1	Level 0	Level $+1$
MTL viscosity, μ (Pa s)	0.2	0.4	0.6
MTL radius of gyration, κ (nm)	0.365	0.73	1.095
Sliding velocity, U (m/s)	10.5	21.0	31.5

checked for the presence of non-random patterns. It is necessary for one of the three parameters μ , κ , U to be held constant at each distinct level (-1 , 0 and $+1$) to formulate a predictive model. However, the choice of constant parameter plays a major role in the accuracy of the predictive model. For example, we choose to keep μ constant at each level by examination of the corresponding residual plots, resulting in three predictive equations that are functions of κ and U . Hence, the parameter to be kept constant in each case was chosen by careful analysis of the residual plots so as to remove any bias.

The predictive fifth order model equation for y has the general form of Eq. 1:

$$y = b_o + b_1x_1 + b_2x_2 + b_{11}x_1^2 + b_{22}x_2^2 + b_{12}x_1x_2 + b_{111}x_1^3 + b_{112}x_1^2x_2 + b_{122}x_1x_2^2 + b_{222}x_2^3 + \dots + b_{22222}x_2^5 \quad (1)$$

To calculate the predicted value of y for forces or stiffnesses (here, $y = P$, Q , K_p , K_Q) first the coefficient vector $b = (x \cdot \dot{x})^{-1} \cdot \dot{x} \cdot y$ is calculated, where x and y are the input factor and output response vectors respectively and denotes

the dot product (DeVor et al. 1992). Here, Eqs. 2, 3 and 4, give the model coefficients for predicting maximum bearing force, P_{max} for three levels of κ (and x_1 , x_2 are the coded values of the varied parameters (here $x_1 = \mu$, $x_2 = U$). In the same way maximum bearing force for three levels of μ and U can be calculated using the coefficients given in ‘‘Appendix 2’’. A fifth order model was proved sufficient to capture the main and confounded effects.

$$P_{max}[\kappa : -1 \text{ order}] = 0.2432\mu U^2 - 0.0144\mu^2 U^2 - 0.0319U^4 + 0.0002\mu^3 U^2 - 0.0002\mu^2 U^3 + 0.044\mu U^4 \quad (2)$$

[Residual error 0.154×10^{-6}]

$$P_{max}[\kappa : 0 \text{ order}] = 0.1701\mu U^2 - 0.01\mu^2 U^2 + 0.0002\mu^3 U^2 \quad (3)$$

[Residual error 0.64×10^{-6}]

$$P_{max}[\kappa : +1 \text{ order}] = -0.0004\mu^4 + 0.1526\mu U^2 - 0.0091\mu^2 U^2 - 0.2867U^4 + 0.0002\mu^3 U^2 - 0.0005\mu^2 U^3 + 0.0219\mu U^4 \quad (4)$$

[Residual error 0.154×10^{-15}]

3 Results and discussion

For the three varying parameters μ , κ , U , the effects of variation from level -1 to $+1$ is shown in Table 6. The comparison is done with the zero level values of P , Q , K_p , K_Q by taking the ratio (in percentage) of total change and zero level value for each of the four parameters. At high shear rate the lubricant behaves like a semi-solid and can withstand bearing and shear forces (Vakis et al. 2011). Viscosity affects mostly the force sustainability capacity of the lubricant, whereas radius of gyration affects the normal and shearing stiffnesses. With the increase of viscosity the lubricant provides more constrain to the penetration. The smaller the κ , the larger the mobile lubricant layer thickness and this mobile lubricant is responsible of increasing

Table 6 Comparison of forces and stiffnesses between -1 and $+1$ levels

Difference between maximum and minimum value	For change of radius of gyration, κ	For change of sliding velocity, U	For change of limiting viscosity, μ
Normal force, P (mN)	3.2 (59.6 %)	2.8 (52.1 %)	5.4 (100.6 %)
Shear force, Q (μN)	0.16 (6.0 %)	0.16 (6.0 %)	0.95 (34.9 %)
Normal stiffness, K_p (N/ μm)	8.4 (228.4 %)	1.9 (51.7 %)	3.7 (100.6 %)
Shear stiffness, K_Q (N/m)	116.13 (133.3 %)	0 (0 %)	0 (0 %)

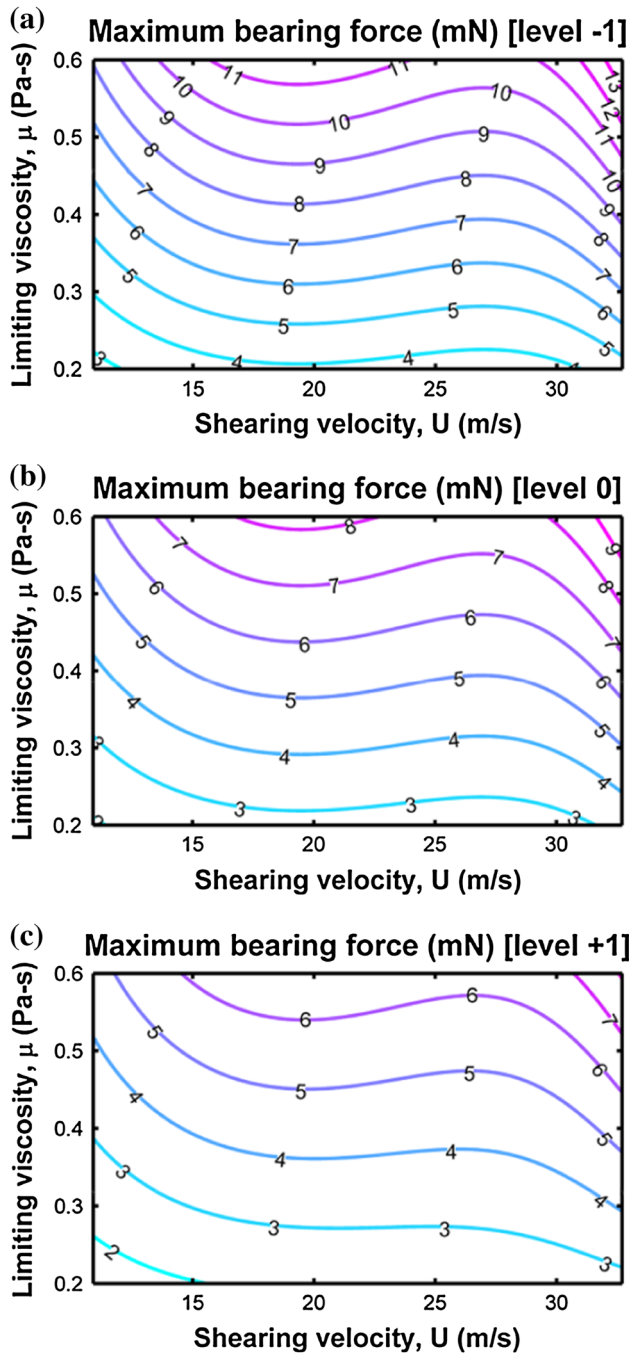


Fig. 7 Parametric plots of the maximum bearing forces for three different levels of radius of gyration κ (case 1)

the lubricant stiffness. All forces and stiffnesses decrease with the increase of radius of gyration. Thus it is important to select a lubricant with lower κ : between the two PFPE lubricants available with κ values of 0.73 and 0.94 nm, the lubricant with $\kappa = 0.73$ nm would be the better choice. With the increase of sliding velocity, the bearing and shear forces, as well as the normal stiffness, increase. The sliding velocity, due to the MTL model formulation, has no effect on the shear stiffness. Physically, this could be attributable to the interfacial slip velocity having reached its maximum value beyond the critical shear rate (Martini et al. 2008). Among the three parameters, the bearing and shear forces are most sensitive to viscosity and they increase with increasing viscosity. As discussed earlier, we want the bearing force to be high so that the lubricant can potentially provide sufficient wear protection to the interface; hence, it is very important to maintain high viscosity.

3.1 Design of experiments/analysis of variance (DOE/ANOVA) results

The maximum bearing forces at the three different levels of μ , κ , U are shown in Figs. 7, 8 and 9. The DOE results can be subdivided into three cases.

- Case 1: Variation of μ and U for three levels of κ
- Case 2: Variation of κ and μ for three levels of U
- Case 3: Variation of κ and U for three levels of μ

3.1.1 Case 1 (DOE analysis for fixed κ)—Fig. 7

In this case μ and U are varied for three levels of κ as shown in Fig. 7. The maximum bearing force increases sharply with increasing limiting viscosity, but with the increase of shearing velocity the increment is negligible compared to the change caused by viscosity. Thus, a change of viscosity plays dominant role. However if that compromises other benefits of PFPE (increasing viscous shear), then the high temperature induced in the slider disk contact needs to be cooled down. A design recommendation is to use a lubricant that will be more resistant to heating. Beyond this, another possibility would be to reduce the average lubricant thickness to allow for faster heat conduction, although this

would potentially compromise other important lubricant properties such as surface coverage.

3.1.2 Case 2 (DOE analysis for fixed U)—Fig. 8

κ and μ are varied for three levels of U , as shown in Fig. 8. The maximum bearing forces decrease with increment of

radius of gyration and increase with increasing limiting viscosity. Also, in this case the effect of μ is more prominent than that of κ . This analysis is done considering that the total thickness of the lubricant is the same and only the bonded lubricant thickness ($=2 \times$ radius of gyration) is varied. Nevertheless the lubricant with lower bonded thickness exhibits better bearing capability.

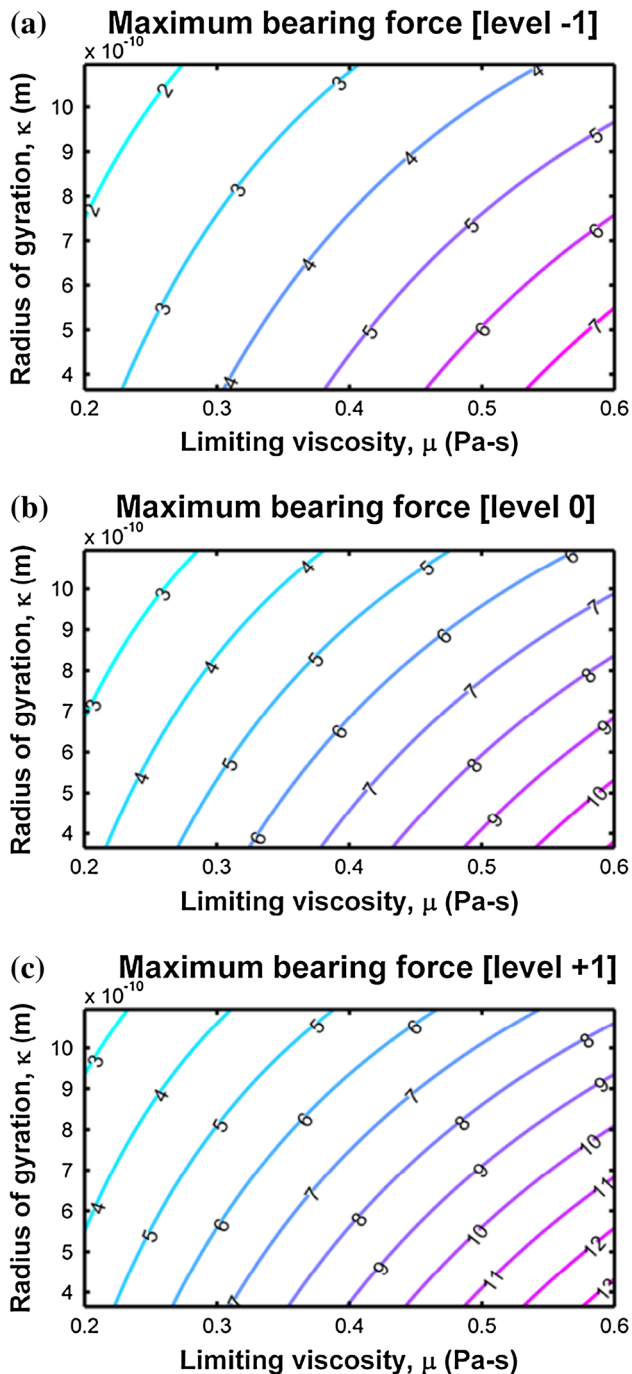


Fig. 8 Parametric plots of the maximum bearing forces for three different levels of shearing velocity U (case 2)

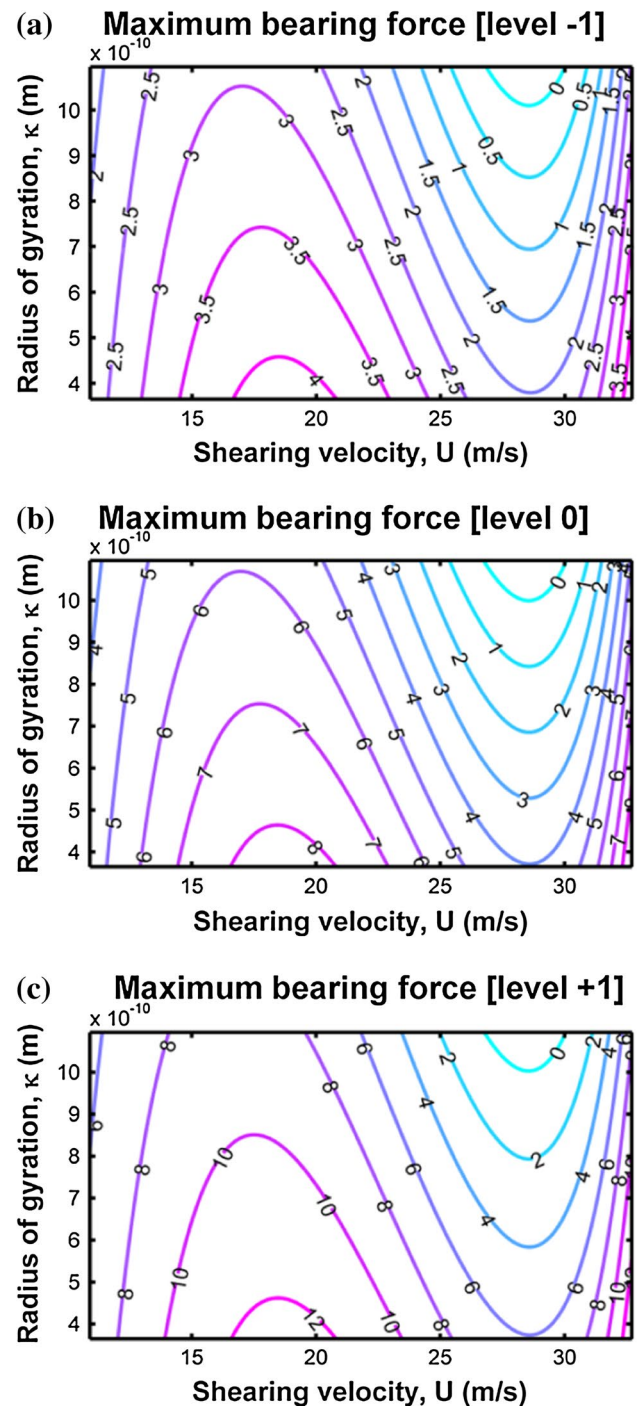


Fig. 9 Parametric plots of the maximum bearing forces for three different levels of limiting viscosity μ (case 3)

3.1.3 Case 3 (DOE analysis for fixed μ)—Fig. 9

In Fig. 9 the variation of κ and U for three levels of μ is shown. The maximum bearing forces decrease with the increase of the radius of gyration. The bearing forces increases with the increase of shearing velocity, however in between it shows complex behavior. In consequence to this the maximum sliding velocity that can be attainable without hindering the read/write performance should be employed.

3.2 Residual analysis

From the residual analysis (given in Eqs. 2, 3, 4, 14, 15, 16, 17, 18, 19), case 1, which is the parametric study with different levels of radius of gyration, gives minimum error, while residuals are randomly oriented for changes of individual parameters. However, if the varying parameter needed for design is μ or U then case 2 or 3 of the study can be used, respectively.

Thus from the predictive models given in Eqs. 2, 3, 4 (for fixed κ), in 14, 15, 16 (for fixed U) and in 17, 18, 19 (for fixed μ) can be employed to find the maximum bearing force in the mobile lubricant layer.

4 Conclusion

Confined MTL layers under high shear rates have viscosity values that are five to eight times of the bulk viscosity at the operating temperature. Based on published research, we used a temperature of the MTL of 90–120 °C, corresponding to an MTL viscosity range of 0.4 ± 0.2 Pas. The bearing and shear forces and stiffnesses were calculated using the MTL model and the bearing stiffnesses are within the expected range, compared to solid surface forces. The force and stiffnesses ascertain reasonable values compared to the literature. A 3^3 full-factorial design was implemented to observe MTL behavior at different levels of μ , κ , and U . From residual analysis, the error was found to be lowest by keeping κ fixed and varying μ and U . A number of response surface plots were obtained through DOE nonlinear regression modeling. It was found that the maximum bearing forces are most sensitive to the increase of limiting viscosity. In comparison, the increment is undetectable for the increase of shearing velocity; whereas, bearing force declines with higher radius of gyration. It is found that it is very important to maintain high viscosity by lowering the temperature of the slider-disk contact using adequate cooling or by employing lubricants with more resistance to heating (i.e., high viscosity of the MTL at elevated temperatures). In this manner, we can increase the bearing forces of the MTL sustainability, which is desirable as it will

enable robust “surf” recording without solid contact and the possibility of wear and catastrophic failures. A lower radius of gyration lubricant is preferable and sliding velocity of 15–20 m/s will have enhanced performance. Hence optimum operating circumstance can be attained for the HDD to accomplish maximum bearing capacity using this analysis.

Acknowledgments The motivation of this work was through a sponsored research program from Seagate Technology LLC, through Grant No. SRA- 32724.

Appendix 1: The MTL model

According to the MTL model, the expressions for normal (P) and shearing (Q) forces are given by Eqs. 5 and 6 respectively. Where P_o and Q_o are the maximum experimental normal and shear forces given by Eqs. 7 and 8. The experimental shearing velocity $U = 200 \mu\text{m/s}$; the radius of spherical shearing probe $R = 102 \mu\text{m}$ (Vakis et al. 2011). Then the critical shear rate is $U/\kappa = 2 \times 10^5/\text{s}$ for $\kappa = 1 \text{ nm}$ (Wood 2002).

$$P_{lube} = P_o \left(\frac{\dot{\gamma}}{\dot{\gamma}_0} \right)^m \tag{5}$$

$$Q_{lube} = m \log \left(\frac{\dot{\gamma}}{\dot{\gamma}_0} \right) + Q_o \tag{6}$$

$$P_o = \frac{6\pi}{5} \mu U \sqrt{\frac{2R^3}{\kappa}} \tag{7}$$

$$Q_o = \frac{16\pi}{5} \mu UR \ln \left(\frac{\kappa}{R} \right) \tag{8}$$

The fitting coefficients m and n are calculated from Eqs. 9 and 10 and can also be obtained from the logarithmic curves of normal and shear forces vs. shear rate.

$$m = \frac{\log \left(\frac{P_{lube,2}}{P_{lube,1}} \right)}{\log \left(\frac{\dot{\gamma}_2}{\dot{\gamma}_1} \right)} \tag{9}$$

$$n = \frac{Q_{lube,2} - Q_{lube,1}}{\log \left(\frac{\dot{\gamma}_2}{\dot{\gamma}_1} \right)} \tag{10}$$

The normal and shear stiffnesses are calculated according to Eqs. 11 and 12. Where the shear rate is found from the expression, U/d_o and this becomes maximum when the solid–solid gap reaches the bonded lubricant thickness (2κ).

$$k_P = \left| \frac{\partial P_{lube}}{\partial d_o} \right| = \frac{mP_o}{U\dot{\gamma}_o^m} \dot{\gamma}^m \tag{11}$$

$$k_Q = \left| \frac{\partial Q_{lube}}{\partial d_o} \right| = \frac{n}{U \ln(10)} \dot{\gamma} \quad (12)$$

$$\dot{\gamma} = \frac{U}{d_o} = \frac{U}{h - 3\sigma - \kappa} \quad (13)$$

Here d_o is the liquid gap. The maximum shear rate is when $d_o = \kappa$, i.e., $h - 3\sigma = 2\kappa$ (when the distance between slider and disk becomes twice the bonded lubricant thickness).

Appendix 2: Regression models

The coefficients for predicting the maximum bearing force for the three levels of U are given in Eqs. 14, 15 and 16.

$$P_{\max}[U : -1 \text{ order}] = -0.0206 \times 10^7 \mu - 0.7135 \times 10^7 \mu^2 - 0.1427 \times 10^7 \kappa^2 \mu^2 \quad (14)$$

$$P_{\max}[U : 0 \text{ order}] = -1.096 \times 10^7 \kappa^3 \quad (15)$$

$$P_{\max}[U : +1 \text{ order}] = 0.0205 \times 10^7 \mu - 1.41 \times 10^7 \mu^2 + 0.1427 \times 10^7 \kappa^2 \mu^2 \quad (16)$$

The coefficients for predicting the maximum bearing force for the three levels of μ is given in Eqs. 17, 18 and 19.

$$P_{\max}[\mu : -1 \text{ order}] = -0.57 \times 10^3 \kappa^2 U^2 + 0.015 \times 10^3 \kappa^3 U^2 \quad (17)$$

$$P_{\max}[\mu : 0 \text{ order}] = -1.12 \times 10^3 \kappa^2 U^2 + 0.03 \times 10^3 \kappa^3 U^2 \quad (18)$$

$$P_{\max}[\mu : +1 \text{ order}] = -1.7 \times 10^3 \kappa^2 U^2 + 0.045 \times 10^3 \kappa^3 U^2 \quad (19)$$

References

- Archard JF (1958) The temperature of rubbing surfaces. *Wear* 2:438–455
- Cho YK, Cai L, Granick S (1997) Molecular tribology of lubricants and additives. *Tribol Int* 30(12):889–894
- Demirel AL, Granick S (1998) Transition from static to kinetic friction in a model lubricated system. *J Chem Phys* 109(16):6889–6897
- Deolalikar N, Sadeghi F (2008) Numerical modeling of mixed lubrication and flash temperature in EHL elliptical contacts. *J Tribol*. doi:10.1115/1.2805429
- DeVor RE, Chang TH, Sutherland JW (1992) Statistical quality design and control: contemporary concepts and methods. Prentice-Hall, Upper Saddle River
- Fisher LR, Israelachvili JN (1979) Direct experimental verification of the Kelvin equation for capillary condensation. *Nature* 277:548–549
- Fukuzawa K, Hayakawa K, Matsumura N, Itoh S, Zhang H (2009) Simultaneously measuring lateral and vertical forces with accurate gap control for clarifying lubrication phenomena at nanometer gap. *Tribol Lett* 37(3):497–505
- Greenwood JA, Williamson JB (1966) Contact of nominally flat surfaces. *Proc R Soc*. doi:10.1098/rspa.1966.0242
- Guo XC, Marchon B, Wang RH, Mate CM, Dai Q, Waltman RJ, Deng H, Pocker D, Xiao QF, Saito Y, Ohtani T (2012) A multidentate lubricant for use in hard disk drives at sub-nanometer thickness. *J Appl Phys* 111:024503
- Hiroshi T, Tagawa N (2012) Adhesion and friction properties of molecularly thin perfluoropolyether liquid films on solid surfaces. *Langmuir* 28:3814–3820
- Karis TE (2009) Lubricants for the disk drive industry. In: Rudnick L (ed) *Lubricant additives: chemistry and applications*, 2nd edn. CRC Press, FL, pp 523–584
- Kogut L, Etsion I (2004) A static friction model for elastic-plastic contacting rough surfaces. *J Tribol T ASME* 126:34–40
- Kunkel GH, Lou H, Macken D, Stoebe TW (2014) Resistance temperature sensors for head-media and asperity detection. Patent No: US 8,737,009 B2
- Lee SC, Polycarpou AA (2005) Microtribodynamics of pseudo-contacting head-disk interfaces intended for 1 Tbit/in². *IEEE Trans Magn* 41(2):812–818
- Lee SC, Strom BD (2008) Characterization of thermally actuated pole tip protrusion for head-media spacing adjustment in hard disk drives. *J Tribol-T ASME* 130(2):022001
- Marchon B, Saito Y (2009) Lubricant design attributes for subnanometer head-disk clearance. *IEEE Trans Magn* 45(2):872–876
- Martini A, Hsu HY, Patankar NA, Lichter S (2008) Slip at high shear rates. *Phys Rev Lett*. doi:10.1103/PhysRevLett.100.206001
- Mate CM, Lorenz MR, Novotny V, Sanders IL, Lin LJ (1989) Tribological studies of storage media by atomic force microscopy. *IEEE GA-7*
- Muller VM, Yushchenko VS, Derjaguin BV (1980) On the influence of molecular forces on the deformation of an elastic sphere and its sticking to a rigid plane. *J Coll Interface Sci* 77(1):91–101
- Persson BNJ (1997) Molecular tribology of lubricants and additives. *Tribol Int* 30(12):889–894
- Rong J, Thomas L, Chong TC (2008) TOF-SIMS analysis for thermal effect study of hard disk lubricant. *Appl Surface Sci* 255(4):1490–1493
- Scarpulla MA, Mate CM (2003) Air shear driven flow of thin perfluoropolyether polymer films. *J chem phys* 118(7):3368–3375
- Seagate technology (2014), What is the normal operating temperature for seagate disk drives? http://knowledge.seagate.com/articles/en_US/FAQ/193771en. Accessed 20 March 2014
- Spikes HA, Olver AV (2009) Compression heating and cooling in elastohydrodynamic contacts. *Tribol Lett* 36(1):69–80
- Stanley HM, Etsion I, Bogoy DB (1990) Adhesion of contacting rough surfaces in the presence of sub-boundary lubrication. *J Tribol* 112(1):98–104
- Suh AY, Polycarpou AA (2005) Adhesive contact modeling for sub-5-nm ultralow flying magnetic storage head-disk interfaces including roughness effects. *J Appl Phys*. doi:10.1063/1.1914951
- Suh AY, Polycarpou AA (2008) Design optimization of sub-5 nm head-disk interfaces using a two-degree-of-freedom dynamic contact model with friction. *Int J Prod Dev* 5(3–4):268–291
- Suh AY, Mate CM, Payne RN, Polycarpou AA (2006) Experimental and theoretical evaluation of friction at contacting magnetic storage slider-disk interfaces. *Tribol Lett* 23(3):177–190
- Vakis AI, Polycarpou AA (2010) Head-disk interface nanotribology for Tbit/in² recording densities: near-contact and contact recording. *J Phys D Appl Phys*. doi:10.1088/0022-3727/43/22/225301
- Vakis AI, Polycarpou AA (2012) Modeling sliding contact of rough surfaces with molecularly thin lubricant. *Tribol Lett* 45(1):37–48
- Vakis AI, Polycarpou AA (2013) An advanced rough surface continuum-based contact and sliding model in the presence of molecularly thin lubricant. *Tribol Lett* 49(1):227–238

- Vakis AI, Lee SC, Polycarpou AA (2009) Dynamic head–disk interface instabilities with friction for light contact (surfing) recording. *IEEE Trans Magn* 45(11):4966–4971
- Vakis AI, Eriten M, Polycarpou AA (2011) Modeling bearing and shear forces in molecularly thin lubricants. *Tribol Lett* 41(3):573–586
- Vakis AI, Hadjicostis CN, Polycarpou AA (2012) Three-DOF dynamic model with lubricant contact for thermal fly-height control nanotechnology. *J Phys D Appl Phys* 45:135402
- Wietzel U (1993) Significance of temperature effects for the behavior of thin lubricant films in an oscillating contact. *Wear* 169(1):59–62
- Wood RW (2002) Recording technologies for terabit per square inch systems. *IEEE Trans Magn* 38(4):1711–1718
- Yeo CD, Sullivan M, Lee SC, Polycarpou AA (2008) Friction force measurements and modeling in hard disk drives. *IEEE Trans Magn* 44(1):157–162
- Zhu Y, Granick S (2004) Superlubricity: a paradox about confined fluids resolved. *Phys Rev Lett*. doi:[10.1103/PhysRevLett.93.096101](https://doi.org/10.1103/PhysRevLett.93.096101)